inventions

MDPI

Article

Several Aspects of Interaction between Chrome and Nanodiamond Particles in Metal Matrix Composites When Being Heated

Vladimir Popov [1,*], Anna Borunova [2], Evgeny Shelekhov [1], Vladimir Cheverikin [1] and Igor Khodos [3]

[1] Department of Physical Metallurgy of Non-ferrous Metals, National University of Science and Technology "MISIS", 119049 Moscow, Russia
[2] Voevodsky Laboratory on Kinetics of Mechanochemical and Free-Radical Reactions, N.N. Semenov Federal Research Center for Chemical Physics of Russian Academy of Sciences, 119991 Moscow, Russia
[3] Laboratory of Electron Microscopy, Institute of Microelectronics Technology and High Purity Materials of Russian Academy of Sciences, 142432 Chernogolovka, Russia
* Correspondence: popov58@inbox.ru

Abstract: The paper considers the development of a technological scheme for preparing metal matrix nanocomposites based on the interaction between nanodiamond reinforcing particles and a chromium matrix when being heated, forming chromium carbide nanoparticles. These carbides are in situ synthesized ceramic reinforcing nanoparticles. The first stage of preparing composites is to obtain composites with the chromium matrix and nanodiamond reinforcing particles. For this purpose, mechanical alloying is used, i.e., processing in planetary mills. The size of a primary nanodiamond particle is 5 nm, but they are combined in agglomerates that are hundreds of micrometers in size. The time of processing in the planetary mill defines the crushing degree of the agglomerates. In this study, processing was carried out for 0.5 h, 2 h, and 4 h. The second stage for obtaining composites with reinforcing particles of chromium carbides is thermal processing. Explorations using the method of differential scanning calorimetry showed that reducing the size of nanodiamond reinforcing particles (by prolonging the time of processing in the planetary mill) leads to a decrease in the initial temperature of the reaction for developing carbides. The worked-out technique for obtaining composites was patented in the Russian Federation (the patent for invention 2772480).

Keywords: metal matrix nanocomposites; nanodiamonds; chromium carbides; mechanical alloying; in situ synthesis

Citation: Popov, V.; Borunova, A.; Shelekhov, E.; Cheverikin, V.; Khodos, I. Several Aspects of Interaction between Chrome and Nanodiamond Particles in Metal Matrix Composites When Being Heated. *Inventions* **2022**, *7*, 75. https://doi.org/10.3390/inventions7030075

Academic Editor: Goshtasp Cheraghian

Received: 9 August 2022
Accepted: 31 August 2022
Published: 2 September 2022

1. Introduction

The use of various carbon nanoparticles (e.g., fullerenes [1,2], nanodiamonds [3–14], nanographite [15,16], etc.) in developing composites with a polymeric or metallic matrix generates substantial interest [17–22]. Chemical interaction between metals and carbonic nanoparticles proceeds differently in comparison with macro-materials [23–25]. This paper considers the interaction between chrome and nanodiamonds in metal matrix composites with a chromium matrix and nanodiamond reinforcing particles. Chromium carbides [26] are divided into stable and metastable types. Stable chromium carbides include $Cr_{23}C_6$, Cr_7C_3 (hP80), and Cr_3C_2 (oP20); metastable chromium carbides include Cr_2C, Cr_3C, CrC, Cr_7C_3 (hP20), and Cr_3C_2 (oC20).

These composites generate interest for several reasons. Chromium is a metal that is widely used in engineering. Substantial amounts of chromium are used in coatings, including electrochemical ones. However, when producing electrochemical chromium coatings, the use of carcinogenic materials cannot be avoided. This fact reduces the attractiveness of such technologies. There are other techniques for applying coatings (e.g., gas dynamics [27,28], frictional cladding [29], etc.). However, to improve the efficiency of

such coatings, when chrome is used, it is necessary to modify the chromium material to improve its wear resistance, durability, etc. This paper considers such a modification of the chromium material using nanoparticles, providing an opportunity to improve the mechanical properties of the material without degrading the quality of its surface.

2. Materials, Equipment, and Methods

For our explorations, commercially available powders of chromium and nanodiamonds were used (Figure 1). The average particle size of chromium powder was 5–10 μm. The size of primary nanodiamond particles was 5 nm, but the nanodiamonds were combined in agglomerates up to hundreds and thousands of micrometers in size. The content of nanodiamond particles in the explored composites was 15% by volume.

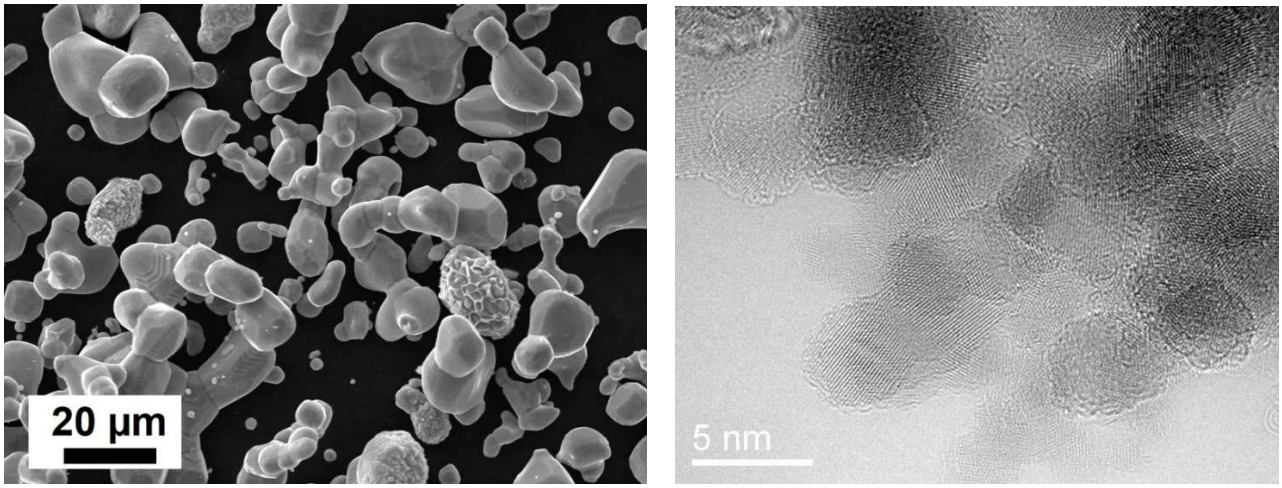

(**a**) (**b**)

Figure 1. Initial materials: (**a**) chromium particles (SEM); (**b**) nanodiamonds (TEM).

To obtain composite granules, mechanical alloying was applied, i.e., co-processing of the composite components in a planetary mill [30–32]. For this purpose, a Pulverisette 6 planetary mono-mill (FRITSCH GmbH, Idar-Oberstein, Germany) was used, with a grinding jar capacity of 80 mL and grinding balls of 5 mm in diameter made of chromium steel. The ratio of the balls' weight to the processed materials' weight was 36:1. The rotation speed was 400 rpm. The processing was implemented in an argon atmosphere for 0.5–4 h (the shut-down period for cooling was not included in the total processing time). The initial and processed materials were examined via X-ray diffraction (XRD), differential scanning calorimetry (DSC), scanning electron microscopy (SEM), and transmission electron microscopy (TEM) methods. X-ray diffraction was carried out using a DRON-3 diffractometer (Saint-Petersburg, Russia) and a D8 ADVANCE Bruker diffractometer (Berlin, Germany) in monochromatic Cu Kα radiation (with a diffracted-beam monochromator), using the EVA phase analysis software package and the PDF-2-2006 database of interplanar distances of crystalline phases. The study of thermal effects during sample heating was implemented on a DSC 404 C Pegasus differential scanning calorimeter manufactured by NETZSCH (Selb, Germany). Measurements were performed in platinum–rhodium crucibles with aluminum oxide inserts under a heating rate of 20 °C·min^{-1}. First, in a tightly sealed chamber of the calorimeter, a vacuum was created, and then the chamber was filled with argon; a sample was placed in the chamber before the creation of the vacuum. A dynamic inert atmosphere (argon; blowdown rate: 50 mL·min^{-1}) was maintained during the measurements. A TESCAN VEGA3 (Brno-Kohoutovice, Czech Republic) scanning electron microscope was used for examining the general appearance of granules and their surface. Transmission electron microscopy studies were performed with JEOL JEM 2100F and JEOL JEM 2100 F/Cs transmission electron microscopes (Akishima, Japan).

3. Results and Discussion

Composite granules are generated as the result of co-processing nanodiamonds with chromium powder. Figure 2 demonstrates the general appearance of the composite granules (chromium + 15% nanodiamonds by volume) after various times of processing by mechanical alloying (SEM images). The average particle size of the primary chromium powder was 5–10 μm. During mechanical alloying, the particles of the processed material were joined and cracked, the nanodiamond agglomerates were fragmented, and the components were mixed. The processing time influences the mixing ratio of the materials, the crushing ratio of the nanodiamond agglomerates, and the size of composite granules.

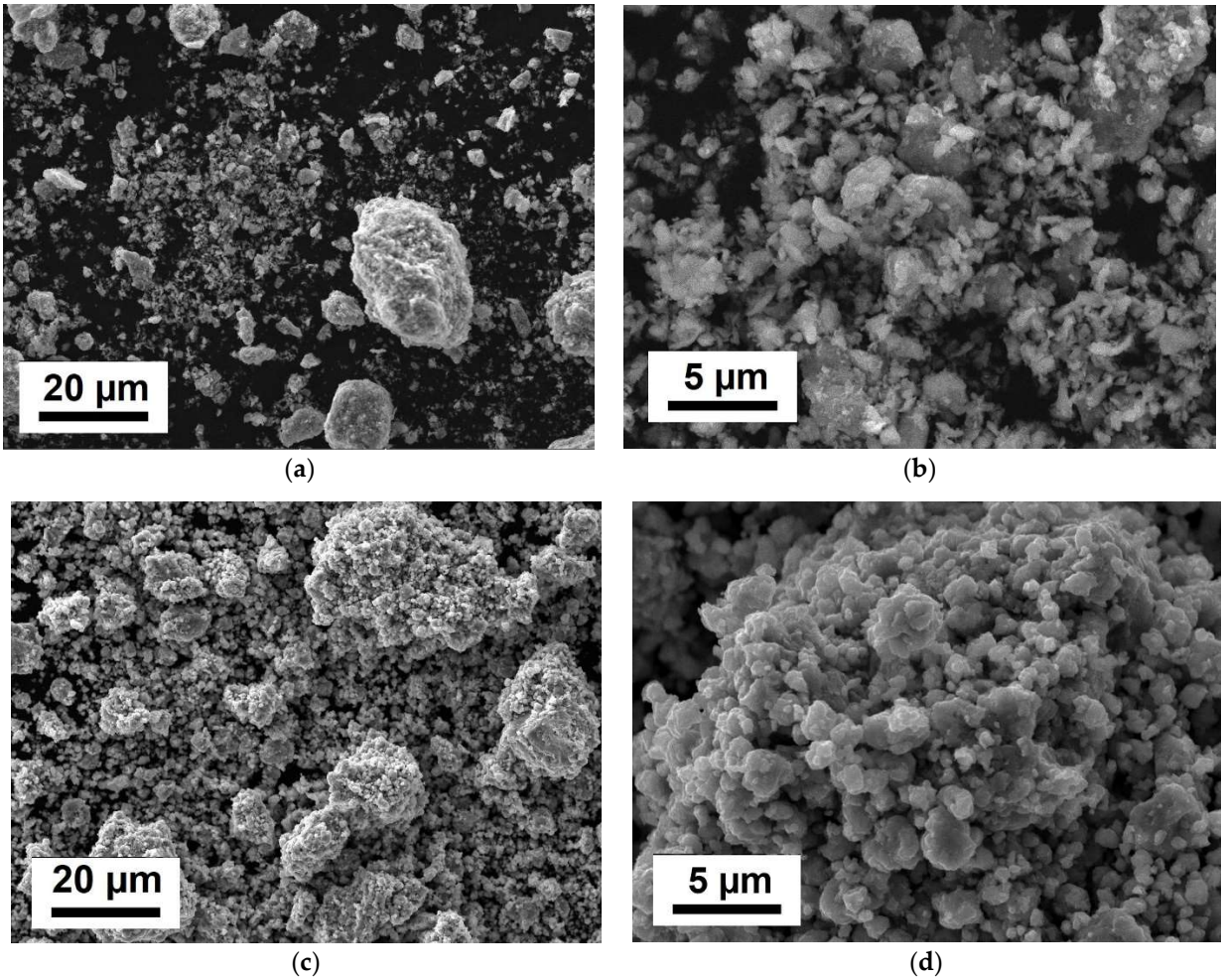

Figure 2. SEM images of the composite (chromium + 15% nanodiamonds) after 0.5 h (**a**,**b**) and 4 h (**c**,**d**) of treatment.

Even after 0.5 h of treatment, the size of the nanodiamond agglomerates was reduced substantially, and they were integrated in the chromium matrix. The sizes of the granules varied from 1 μm to 30 μm (Figure 2a,b). The longer the processing period, the more homogeneous the structure of the composite granules. After processing for 4 h (Figure 2c,d), the fine fraction was reduced; the size of granules was 20–30 μm, but the granules consisted of finer fragments, which is characteristic of the chromium material.

It is impossible to identify crushed nanodiamond agglomerates in mixtures with metals using X-ray diffraction methods (the reason for this is explained in [33,34]). The presence of nanodiamonds can be proven using the synchrotron radiation or transmission electron microscopy methods. Figure 3 shows the electron diffraction pattern obtained when examining the composite (chromium + 15% nanodiamonds by volume) after 2 h of

processing using transmission electron microscopy. Diffraction rings from nanodiamonds (111), (211), (311), along with single reflexes from the chromium material (110), (200), (211), etc., can be seen clearly. It is worth noting that the location of the reflexes from chrome (110) coincides with the ring from nanodiamonds (111). The presence of diffraction rings from nanodiamonds points to the fact that at this stage the nanodiamonds were not transformed into the graphitic material, and did not react with chromium, forming carbides, and reducing the size of the chromium particles substantially (chromium was present in the examination zone not in the form of monocrystal, but in the form of polycrystal).

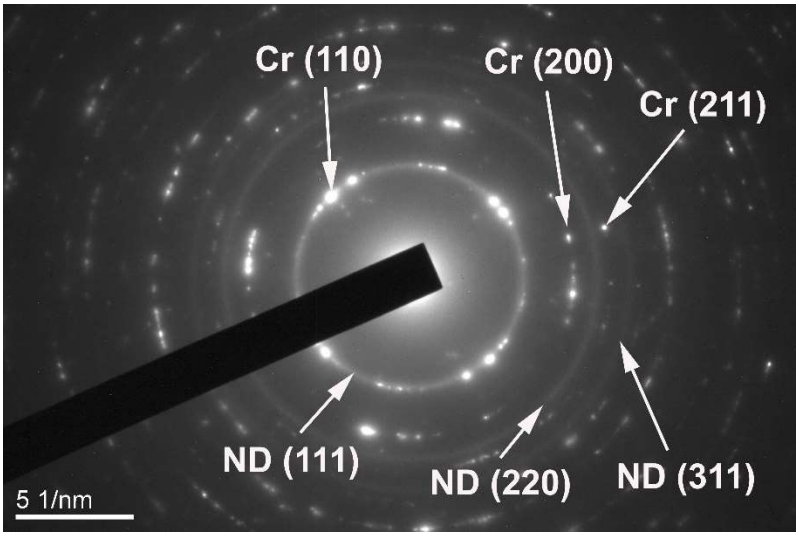

Figure 3. Electron diffraction pattern obtained when examining the composite (chromium + 15% nanodiamonds by volume).

To obtain chromium carbides in industry, thermal processing at temperatures of 1150–1600 °C is used. From previous data, it has been established that using mechanical alloying decreases the necessary level of temperature—for example, to 1000 °C [35]. There is a hypothesis that the starting temperature of the chemical reaction for the formation of carbides will be decreased substantially if the reacting carbonic particles are reduced in size (especially in the nanodimensional area) [23–25,36]. To justify this hypothesis in terms of the chromium + nanodiamonds combination, mechanical alloying of the mixture (chromium powder and nanodiamonds) was carried out for various processing times in the planetary mill (0.5 h, 2 h, and 4 h). The longer the processing time, the greater the fragmentation of nanodiamond agglomerates (i.e., carbonic particles will be reduced in size). The sizes of the crushed nanodiamond agglomerates were assessed using transmission electron microscopy. After processing for 0.5 h, most of the crushed agglomerates were 100–200 nm in size. Increasing the processing time to 2 h further reduced the size of the nanodiamond agglomerates to 30–50 nm. After processing for 4 h, the nanodiamond agglomerates were fragmented substantially, reducing them to 10 nm in size. The size of the primary nanodiamond particles was 5 nm.

Thermal effects under heating were examined using differential scanning calorimetry. Experiments showed that the longer the processing time, the lower the starting temperature of the chemical reaction for generating chromium carbides (Figure 4).

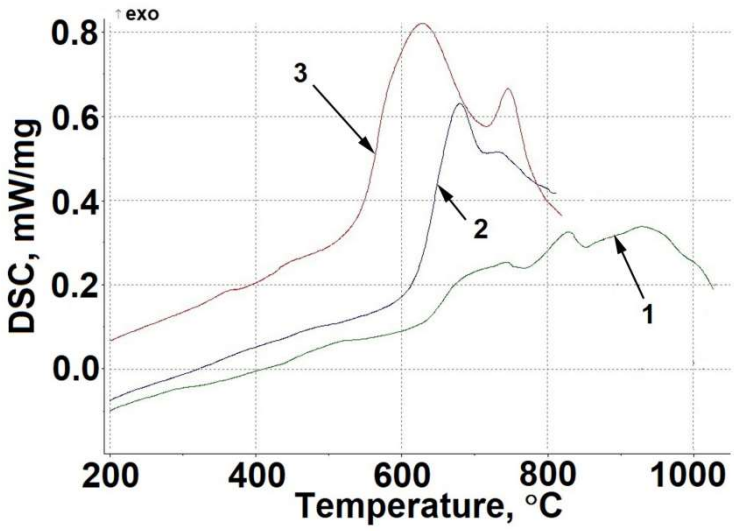

Figure 4. Results of the DSC study of "chromium + 15% nanodiamonds" composites: (1) after 0.5 h; (2) after 2 h; (3) after 4 h.

As already noted, the processing time in the planetary mill defines the crushing ratio of the nanodiamond agglomerates. Thus, the main reason for this decrease in the initial temperature for generating carbides is undoubtedly the reduction in the size of the carbonic particles (nanodiamonds). For example, for the composite (chromium + 15% nanodiamonds by volume), after being processed for 0.5 h, the initial temperature of the chemical reaction for generating chromium carbides was 630 °C; after being processed for 2 h, the starting temperature of the reaction between chromium and the carbonic material was decreased to 600 °C, while mechanical alloying for 4 h decreased the starting temperature of the chemical reaction for generating chromium carbides to 520 °C.

The decrease in the starting temperature of the chemical reaction for generating chromium carbides, when heating the mixture of the chromium material with carbonic nanoparticles (nanodiamonds), is very important for several reasons. On the one hand, these explorations set the temperature interval of the working efficiency for the chromium + nanodiamonds composite. On the other hand, the temperature conditions for generating chromium carbides are set. The knowledge that carbides can be generated even at 520 °C provides an opportunity to substantially reduce the energy consumption for obtaining these materials and the cost of the used equipment, and to extend the operational life of the equipment.

The synthesis of chromium carbides can be proven with X-ray diffraction methods when the samples are heated. Figure 5 shows the X-ray diffraction pattern of the DSC examinations when being heated to 690 °C. The arrows indicate peaks of chromium; vertical lines represent the chromium carbide Cr_7C_3. The unmarked peaks are associated with chromium oxide (oxygen is adsorbed with air in the initial powder; moreover, argon, which is used for the chamber blowdown, also has oxygen remnants, etc.).

Various annealing temperatures and various contents of carbonic reinforcing particles in the composite lead to the formation of various carbides, including metastable ones.

The study of the electron diffraction patterns (obtained via transmission electron microscopy) of the composite during annealing showed the total absence of diffusion rings from the nanodiamonds. Only reflexes from chromium carbides and chromium were observed. This suggests that all of the nanodiamonds reacted, forming chrome carbides. The composite material consisted of the chromium matrix and reinforcing particles of the chromium carbide. The worked-out technique for obtaining the composite material using in situ synthesis of reinforcing carbide particles directly in the chromium matrix was patented in the Russian Federation [37].

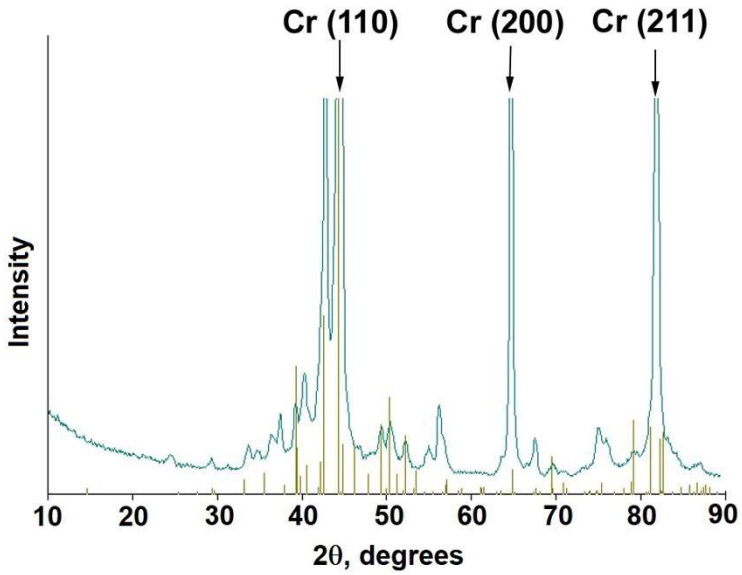

Figure 5. X-ray diffraction patterns from the composite "Cr+15% ND" after annealing at 690 °C. Arrows: chromium; vertical lines: chromium carbide (Cr_7C_3).

4. Conclusions

In metal matrix composites (initial materials: chromium and nanodiamonds), our specific findings were as follows: (i) the duration of the mechanical alloying process has an influence on the typical size of the remaining nanodiamond agglomerates; (ii) the nanodiamonds do not react with the chromium during the milling phase, but persist as nanodiamonds; (iii) the temperature upon heating at a constant rate of 20 K/min at which the massive conversion from nanodiamonds to chromium carbide begins was reduced from 690 °C (after milling for 0.5 h) to 520 °C (after milling for 4 h)—the smaller the size of the carbonic particles, the lower the starting temperature of synthesis.

5. Patents

Popov, V.A. Composite material and its manufacturing method. Patent of the Russian Federation 2,772,480, Bul.14, 2022.

Author Contributions: Conceptualization, methodology, writing and editing, resources, V.P.; investigation (mechanical alloying), A.B.; investigation (X-ray diffraction) E.S.; investigation (scanning electron microscopy), V.C.; investigation (transmission electron microscopy), I.K. All authors have read and agreed to the published version of the manuscript.

Funding: This research received no external funding.

Institutional Review Board Statement: Not applicable.

Informed Consent Statement: Not applicable.

Data Availability Statement: Not applicable.

Acknowledgments: The authors are grateful to B. Senatulin and A. Egorov for assistance in this study.

Conflicts of Interest: The authors declare no conflict of interest.

References

1. Dastjerdi, S.; Akgöz, B. On the statics of fullerene structures. *Int. J. Eng. Sci.* **2019**, *142*, 125–144. [CrossRef]
2. Bhardwaj, J.; Vishnoi, R.; Sharma, G.D.; Asokan, K.; Singhal, R. Mapping the local structure of fullerene C60 and Cu–C60 nanocomposite thin films by gamma rays irradiation. *Mater. Chem. Phys.* **2020**, *252*, 123192. [CrossRef]
3. Chernysheva, M.G.; Sinolits, A.V.; Votyakova, V.S.; Popov, A.G.; Badun, G.A. Preparation and properties of Miramistin–hyaluronic acid coatings on the nanodiamond surface. *Mendeleev Commun.* **2022**, *32*, 501–503. [CrossRef]

4. Kuznetsov, V.L.; Aleksandrov, M.N.; Zagoruiko, I.V.; Chuvilin, A.L.; Moroz, E.M.; Kolomiichuk, V.N.; Likholobov, V.A.; Brylyakov, P.M.; Sakovitch, G.V. Study of Ultra Disperse Diamond Obtained Using Explosion Energy. *Carbon* **1991**, *29*, 665–668. [CrossRef]
5. Basso, L.; Cazzanelli, M.; Orlandi, M.; Miotello, A. Nanodiamonds: Synthesis and Application in Sensing, Catalysis, and the Possible Connection with Some Processes Occurring in Space. *Appl. Sci* **2020**, *10*, 4094. [CrossRef]
6. Mochalin, V.N.; Shenderova, O.; Ho, D.; Gogotsi, Y. The properties and applications of nanodiamonds. *Nat. Nanotechnol* **2012**, *7*, 11–23. [CrossRef]
7. Balakin, S.; Dennison, N.R.; Klemmed, B.; Spohn, J.; Cuniberti, G.; Römhildt, L.; Opitz, J. Immobilization of Detonation Nanodiamonds on Macroscopic Surfaces. *Appl. Sci.* **2019**, *9*, 1064. [CrossRef]
8. Tinwala, H.; Wairkar, S. Production, surface modification and biomedical applications of nanodiamonds: A sparkling tool for theranostics. *Mater. Sci. Eng. C* **2019**, *97*, 913–931. [CrossRef]
9. Mironov, E.; Koretz, A.; Petrov, E. Detonation synthesis ultradispersed diamond structural properties investigation by infrared absorption. *Diam. Relat. Mater.* **2002**, *11*, 872–876. [CrossRef]
10. Volkov, D.S.; Proskurnin, M.A.; Korobov, M.V. Elemental analysis of nanodiamonds by inductively-coupled plasma atomic emission spectroscopy. *Carbon* **2014**, *74*, 1–13. [CrossRef]
11. Krueger, A.; Boedeker, T. Deagglomeration and functionalisation of detonation nanodiamond with long alkyl chains. *Diam. Relat. Mater.* **2008**, *17*, 1367–1370. [CrossRef]
12. Shvidchenko, A.V.; Dideikin, A.T.; Zhukov, A.N. Counterion condensation in hydrosols of single-crystalline detonation nanodiamond particles obtained by air annealing of their agglomerates. *Colloid J.* **2017**, *79*, 567–569. [CrossRef]
13. Shvidchenko, A.V.; Eidelman, E.D.; Vul, A.Y.; Kuznetsov, N.M.; Stolyarova, D.Y.; Belousov, S.I.; Chvalun, S.N. Colloids of detonation nanodiamond particles for advanced applications. *Adv. Colloid Interface Sci.* **2019**, *268*, 64–81. [CrossRef] [PubMed]
14. Stelmakh, S.; Skrobas, K.; Gierlotka, S.; Palosz, D. The shape and surface structure of detonation nanodiamond purified in oxidizing chemical environment. *Diam. Relat. Mater.* **2021**, *113*, 108286. [CrossRef]
15. Kırgız, M.S. Green cement composite concept reinforced by graphite nano-engineered particle suspension for infrastructure renewal material. *Compos. Part B Eng.* **2018**, *154*, 423–429. [CrossRef]
16. Parvizi, S.; Ahmadi, Z.; Zamharir, M.J.; Asl, M.S. Synergistic effects of graphite nano-flakes and submicron SiC particles on the characteristics of spark plasma sintered ZrB2 nanocomposites. *Int. J. Refract. Met. Hard Mater.* **2018**, *75*, 10–17. [CrossRef]
17. Gong, H.; Shao, W.; Ma, W.; Cui, Z. Absorption properties of a multilayer composite nanoparticle for solar thermal utilization. *Opt. Laser Technol.* **2022**, *150*, 107914. [CrossRef]
18. Elsherbini, A.M.; Sabra, S.A. Nanoparticles-in-nanofibers composites: Emphasis on some recent biomedical applications. *J. Control. Release* **2022**, *348*, 57–83. [CrossRef]
19. Liu, W.; Liu, Z.; Guo, Z.; Xie, W.; Tang, A.; Huang, G. A Computational Model for Characterizing Electrical Properties of Flexible Polymer Composite Filled with CNT/GNP Nanoparticles. *Mater. Today Commun.* **2022**, *32*, 104177. [CrossRef]
20. Islam, A.; Sharma, V.K.; Mausam, K. An analytical study of nano carbon materials for developing metal matrix nano composites. *Mater. Today Proc.* **2021**, *45 Pt 2*, 2867–2870. [CrossRef]
21. Reddy, S.N.; Manohar, H.S.; Anand, S.N. Effect of carbon black nano-fillers on tribological properties of Al6061-Aluminium metal matrix composites. *Mater. Today Proc.* **2020**, *20 Pt 2*, 202–207. [CrossRef]
22. Tan, W.; Jiang, X.; Shao, Z.; Sun, H.; Fang, Y.; Shu, F. Fabrication and mechanical properties of nano-carbon reinforced laminated Cu matrix composites. *Powder Technol.* **2022**, *395*, 377–390. [CrossRef]
23. Popov, V. The impact of the diamond reinforcing particle size on their interaction with the aluminum matrix of composites in the course of heating. *Surf. Interface Anal.* **2018**, *50*, 1106–1109. [CrossRef]
24. Popov, V.; Borunova, A.; Senatulin, B.; Shelekhov, E.; Kirichenko, A. Peculiarities of fullerenes and carbon onions application for reinforcing the aluminum matrix in the metal matrix composites. *Surf. Interface Anal.* **2020**, *52*, 127–131. [CrossRef]
25. Popov, V.; Borunova, A.; Shelekhov, E.; Khodos, I.; Senatilin, B.; Matveev, D.; Versinina, E. Peculiarities of chemical interaction of some carbon nanoreinforcements with aluminum matrix in metal matrix composite (MMC). *Mater. Sci. Eng. Technol.* **2022**, *53*, 602–607. [CrossRef]
26. Hirota, K.; Mitani, K.; Yoshinaka, M.; Yamaguchi, O. Simultaneous synthesis and consolidation of chromium carbides (Cr_3C_2, Cr_7C_3 and $Cr_{23}C_6$) by pulsed electric-current pressure sintering. *Mater. Sci. Eng. A* **2005**, *395*, 154–160. [CrossRef]
27. Tripathy, S.; Behera, A.; Pati, S.; Roy, S. Corrosion resistant nickel coating on mild steel by cold gas dynamic spraying. *Mater. Today Proc.* **2021**, *46 Pt 10*, 4395–4399. [CrossRef]
28. Zhang, Y.; Wang, Q.; Chen, G.; Ramachandran, C.S. Mechanical, tribological and corrosion physiognomies of CNT-Al metal matrix composite (MMC) coatings deposited by cold gas dynamic spray (CGDS) process. *Surf. Coat. Technol.* **2020**, *403*, 126380. [CrossRef]
29. Belevskiy, L.; Popov, V.; Tulupov, S.; Smirnov, O. Enhancement of Reliability of Machines and Materials by Friction Plating. *Adv. Mater. Res.* **2009**, *59*, 46–50. [CrossRef]
30. Garbade, R.R.; Dhokey, N.B. Effect of mechanical alloying of Ti and B in pre alloyed gas atomized powder on carbide dispersed austenitic matrix of Iron based hardfacing alloy. *Mater. Charact.* **2022**, *191*, 112134. [CrossRef]
31. Suryanarayana, C. Mechanical alloying and milling. *Prog. Mater. Sci.* **2001**, *46*, 1. [CrossRef]
32. Benjamin, J.; Volin, T. The mechanism of mechanical alloying. *Metall. Trans.* **1974**, *5*, 1929. [CrossRef]

33. Popov, V. X-ray micro-absorption enhancement for non-agglomerated nanodiamonds in mechanically alloyed aluminium matrix composites. *Phys. Status Solidi A* **2015**, *212*, 2722–2726. [CrossRef]
34. Popov, V.; Többens, D.; Prosviryakov, A. Identification of non-agglomerated nanodiamonds inside metal matrix composites by synchrotron radiation. *Phys. Status Solidi A* **2014**, *211*, 2353–2358. [CrossRef]
35. Zhao, Z.; Hu, W. Synthesis and characterization of chromium carbide nanopowders processed by mechanical alloying assisted microwave heating route. *Int. J. Refract. Met. Hard Mater.* **2016**, *58*, 206–210. [CrossRef]
36. Popov, V.; Prosviryakov, A.S.; Senatulin, B.R.; Shelekhov, E.V.; Vershinina, E.V. Study of composites with nanodiamond reinforcing particles. In Proceedings of the XV International Conference on Thermal Analysis and Caloremetry in Russia (RTAC-2016), Sankt-Petersburg, Russia, 19–23 September 2016.
37. Popov, V. Composite Material and Its Manufacturing Method; Bul.14, 20.05.2022. Patent of Russian Federation 2,772,480, 1 February 2022.